Rethinking mask strategies for high vertical resolution grayscale lithography

Gaby Bélot, Aurélien Fay, Elodie Sungauer, Ujwol Palanchoke, Sébastien Bérard-Bergery, Cécile Gourgon

Rethinking Mask Strategies For High Vertical Resolution Grayscale Lithography

Gaby Bélot[b], Aurélien Fay[a], Elodie Sungauer[b], Ujwol Palanchoke[a], Sébastien Bérard-Bergery[b], and Cécile Gourgon[c]

[a]Univ. Grenoble Alpes, CEA, Leti, F-38000 Grenoble, France
[b]STMicroelectronics, 850 rue Jean Monnet, 38926 Crolles Cedex, France
[c]Université Grenoble Alpes, CNRS, CEA/LETI-Minatec, Grenoble INP, LTM, 17 Rue des Martyrs, Grenoble 38054, France

ABSTRACT

Grayscale PhotoLithography (GPL) enables the patterning of various 3D microstructures in a single lithography step with high throughput. For various 3D optical filtering devices to be functional, high vertical resolution and accuracy are key factors. This precision can, in part, be improved by an adapted mask design construction when using GPL as the 3D patterning method. Here we study different mask design approaches to achieve high resolution staircase like structures patterning using GPL.

We found that by using different design flavors, we enlarge the range of available densities for grayscale applications. A relevant design choice also allows us to increase the theoretical vertical resolution enough so that the remaining limitations come not from the mask itself but from the process. The Mask Error Enhancement Factor (MEEF) is also shown to be improvable by tuning the dose sensibility of the design.

Keywords: grayscale lithography, mask variability, 3D patterning, optical devices, vertical resolution

1. INTRODUCTION

In the world of 3D micro-patterning, numerous methods can be found throughout the litterature.[1] If some of them are found to offer a better resolution (i.e. direct write methods such as LASER or e-beam lithography[2] or multiphotons lithography[3]), others are more suitable for mass manufacturing (i.e. grayscale photolithography[4]). The ascent of needs for an efficient compromise between these two factors tends to feed further studies, i.e. for applications in optical devices. Microlenses have been at the center of the 3D patterning world for years, yet the rise of demands for optical filtering devices have raised new challenges.[5] For such applications, a high vertical resolution is often required and adding to the constraints (3D structures dimensions, rugosity, throughput, integration, materials...)

Grayscale PhotoLithography (GPL) is found to be among the best industrial contestants for 3D micro-patterning. This method relies on classical photolithography tools to perform a high throughput fabrication of three dimensional patterns. If this performance in productivity puts GPL before direct write methods like e-beam lithography or direct LASER writing for mass-manufacturing, the other side of the coin implies a weaker resolution. Indeed, GPL resolution on its lateral dimensions is restrained by the optical influence radius. Therefore, the method is currently limited to micrometric objects. The idea behind GPL is to rely on a low contrast photoresist which allows, for different exposure doses inside its transition region, to obtain different resist height post-development. The exposition modulation is obtained by the resort to binary masks composed of sub-resolution features (SRF). The SRF dictate the mask local chromium density and therefore its transmission. In the end, a shaping of the aerial image beneath the mask occurs, without printing the mask patterns in the underlying photoresist (Fig. 1).

One main difference between classical and sub-resolution binary masks are the latter to be less intuitive. Since the mask chromium patterns are not exact replica of what will be printed in the photoresist, linking a

Send correspondence to Gaby Bélot: gaby.belot@st.com

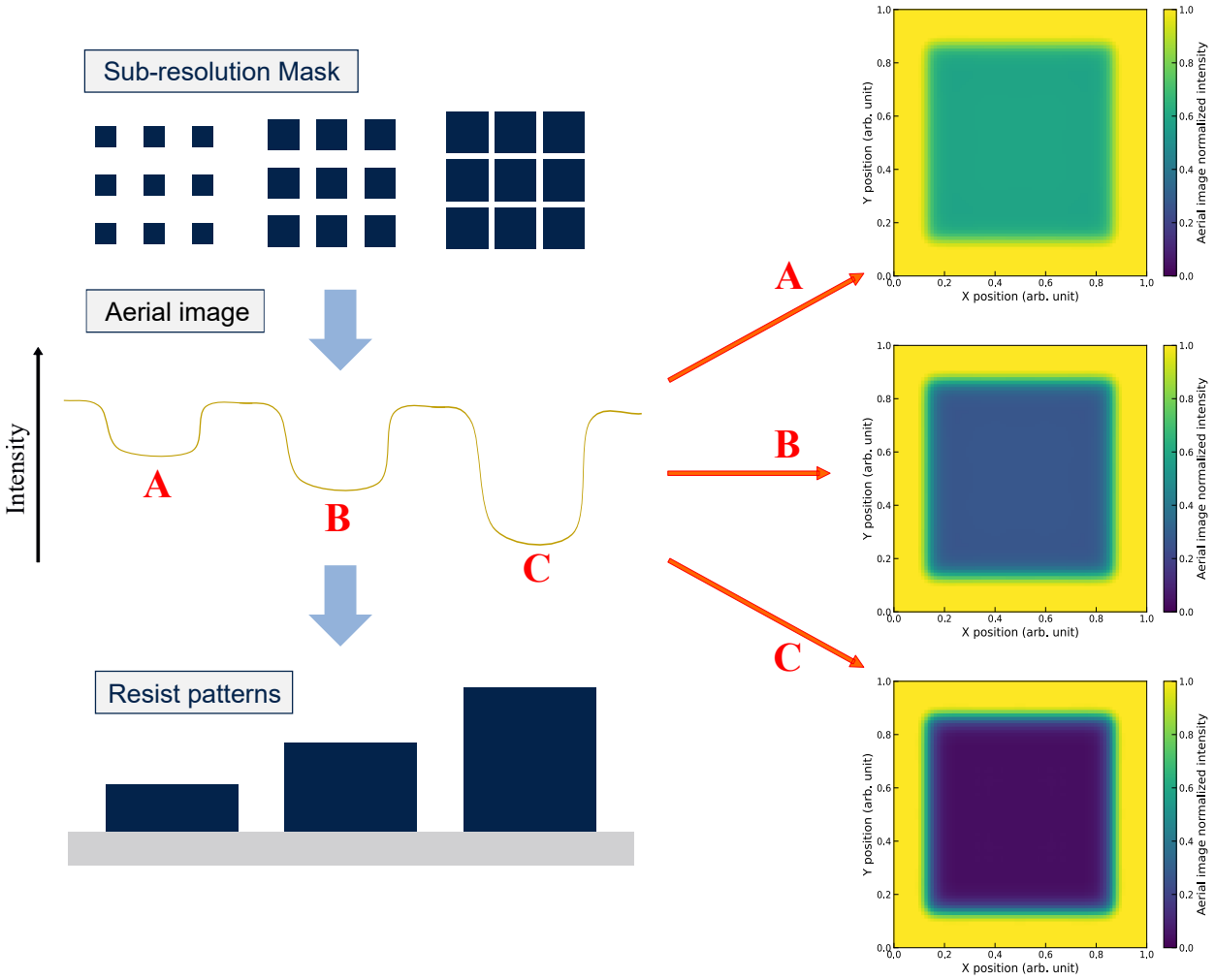

Figure 1: Principle of grayscale photolithography : a mask composed of sub-resolution features is exposed, resulting in a 3D shaping of the aerial image. The recourse to a low contrast photoresist therefore allows 3D patterning

mask design to the associated 3D shape can become quite laborious. Usually, a SRF design strategy is fixed and numerical tools perform the mask construction, relying on simulations.[6,7] Here, we call design strategy the method chosen to arrange together the SRF and obtain the right transmitted intensity map : pitch, position of the features, features shape, features size... If the recourse to binary masks is what gives GPL a head start when it comes to high throughput, it also induces well known issues such as Mask Rule Check (MRC) limitations or Mask Error Enhancement Factor (MEEF).[8] However, a strength of this method is also the available flexibility on the mask patterns. Indeed, for a given 3D target, different mask design strategies can be used to obtain the same response in the resist. The only rules for the mask data preparation are for the mask to be composed of SRF, to offer the desired density gradient and to be manufacturable.

The purpose of this work is to determine a grayscale binary mask design strategy able to enlarge the realm of what can currently be done by GPL. The study vehicle is the fabrication of the cavities for multiple Fabry-Perot interferential filters used for multispectral imaging. Such devices come in the shape of pillars or staircase like structures (Fig.2) and require different cavities heights depending on the filtered wavelengths. Equation 1 gives

the filtered wavelength depending on the cavity thickness : for multispectral imaging, the maximum number of filtered wavelengths is often desired.

$$\lambda \approx \frac{h}{2n} \tag{1}$$

With λ the filtered wavelength, h the cavity thickness and n the cavity material refractive index.

However, multiplying the Fabry-Perot filters implies a high control over the vertical component to perform high quality filtering and prevent overlaps between filters. Typically, a vertical resolution < 5 nm is relevant regarding the transmission. However, this value can become even smaller for a small $\Delta\lambda$ between two filtered wavelength, requiring a smaller Δh between two channels and high control over the patterned channels height. Therefore, the stakes are double during the mask data preparation : on one hand, the chosen strategy must offer an enhanced vertical resolution. On the other hand, the will is also to improve the grayscale patterning response to mask variabilities (MEEF). The limitations due to MRC (Mask Rules Check) are also assessed and shown to be highly reducible depending on the strategy.

In this paper, we will first present a modelisation methodology of our photoresist contrast curve. Producing such a model allows to create a relation between the mask chromium density and the post-lithography resist height. Then, mask considerations for high vertical resolution will be discussed. Especially, the resort to various SRF and pitch modulations are investigated. Finally, the impact of this new considerations on the MEEF is studied and used to isolate the most efficient mask strategy.

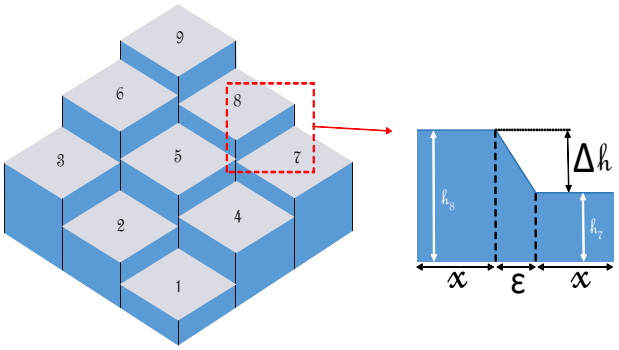

Figure 2: Principle of multiple cavities with varying heights

2. CONTRAST CURVE MODEL

As mentioned previously, for a fixed process, the remaining resist height of grayscale patterned structures is controlled by the mask chromium density. We restrict our study to a precise control over our stairs structures height : due to an assumed large horizontal footprint of the stairs (> 10 µm), the size of the transition between two of them (ϵ on Fig.2) is considered negligible. Therefore, a contrast curve approach is sufficient for the mask data preparation, the contrast curve being the expression of the resulting resist height in function of the received effective dose (light effectively arriving at the surface of the resist, depending on the stepper dose and the mask chromium density).

The first step is then to produce an efficient model of the photoresist contrast curve, directly linking the exposure dose (stepper input dose) and the local mask chromium density to the resulting resist height. Such a compact modelling of the contrast curve only needs two inputs : a model form and experimental data to fit.

2.1 Mathematical model

The goal of the mathematical model is to give a formula linking the final resist height to both the exposure dose and the mask chromium density :

$$h_{resist} = f(Dose_{exposure}, Dens) \tag{2}$$

One way of looking at it to simplify the problem is to reduce the number of unknowns : we can either fix one of them (i.e. work with a single exposure dose), or we can express both the exposure dose and the chromium density under a single variable : the aforementioned effective dose. The second option will be prefered to keep the most flexibility :

$$h_{resist} = f(Dose_{eff}) \tag{3}$$

With the effective dose being the aerial image normalized intensity (I) scaled by the stepper exposure dose :

$$Dose_{eff} = I_{AerialImage}(Dens) * Dose_{exposure} \tag{4}$$

We obtained the aerial images normalized intensities via a Fraunhofer optical model[6] (Fig.3a), allowing us to calculate the effective dose for each exposure dose (Fig.3b).

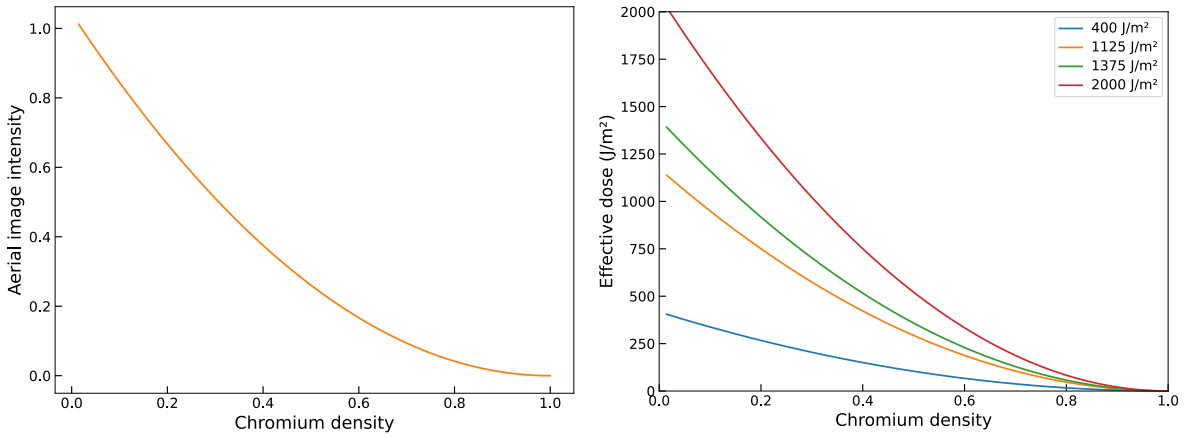

(a) (b)

Figure 3: (a) Evolution of the normalized aerial image values versus mask chromium density. (b) Resulting effective dose vs density for four exposure doses.

The last step is to find an adapted function $f(Dose_{eff})$. For this purpose, we used an order 3 polynomial expression (Eq.5) fitted on experimental data, where e_k are the fit parameters :

$$h_{resist} = \sum_{k=0}^{3} e_k * Dose_{eff}^k \tag{5}$$

2.2 Calibration of the model on experimental profiles

To perform the calibration of the previously established model, experimental data were acquired as follows :

- The illumination is done using a Canon i-line FPA-5510iZ stepper with a numerical aperture of 0.57 and a coherence of 0.7. As for the photoresist, 1.6 µm of JSR-MFR-530 was coated. The development and baking of the resist were done using the supplier best known methods.
- An existing GPL mask was used, it is composed of an arrangement of unitary designs
- Each unitary design answers to the structure presented in Fig.4 : chromium square dots are arranged on a grid with a constant pitch = 330 nm in both directions. The size of the dots is decreasing from one unitary design to another from 300 nm to 40 nm. Therefore, the chromium density is getting lower as we go from a design to another, from 82.6% to 1.5%. Each unitary design has a 40 µm * 3 mm footprint and the space between two designs is 20 µm.

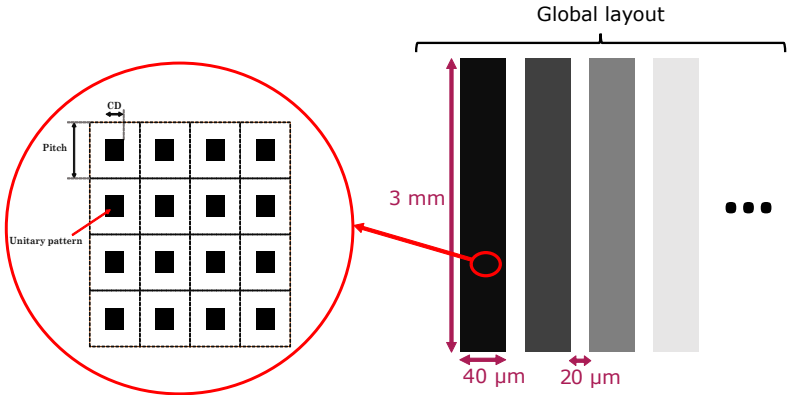

Figure 4: Mask design strategy used for the experimental data. The global layout (right) is an arrangement of 40 µm*3mm unitary designs separated by 20 µm. The unitary designs (left) are an arrangement of square dots on a grid of fixed pitch. The size of the dots modify the chromium density. The chromium density is decreasing from left to right.

- The resulting resist profile of the whole layout is stairs of decreasing heights. These stairs were measured using a mechanical profilomer KLA HRP340. One of the scans is shown on Fig.5.
- The scans were performed on 8 wafers presenting different exposure dose conditions. The measure was realized on multiple positions on each wafer and averaged. Such a methodology was chosen to avoid the profiles degradation due to non-uniformities. Also, our goal is to calibrate a model to predict the behavior of the contrast curve for a wide dose range for more flexibility.

Once the data acquired, a polynomial order 3 fit was performed for one of the dose (700 J/m²). Each other dose was then used as model verification data. The simulated contrast curves using [5] and [4] for each dose are displayed on Fig.6. Various observations are possible upon these results :

- The modelisation is efficient from 700 to 2000 J/m², with an exception for high densities at 2000 J/m² : due to the experimental data lacking at densities higher than 0.83, the fit method is less efficient. This limit in densities comes from MRC limitations and the mask design strategy. This will be discussed later in this paper.

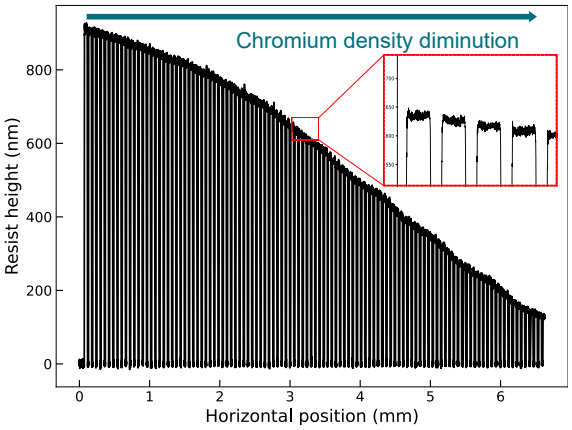

Figure 5: Mechanical profilometer scan of the resulting experimental profile

- A progressive deviation of the experimental data from the model is observable for the lower doses, at which the dose-to-clear is not met. This behavior might be explained by being in another regime due to very short shutter opening time. However, no experimental proof of this theory is available at the moment.
- Periodic waviness is visible on the experimental profiles, especially for low pillars (high consumed resist), and is not predicted by the model. This effect has been linked to the light reflected by the underlayer and the resulting standing waves.

Overall, this compact contrast curve modelisation is satisfying over the working dose range by adopting a mean behavior around the standing waves oscillations. For a better fit however, rigorous simulations are mandatory. The next step is to determine the most efficient mask SRF strategy to "browse" the contrast curve. Indeed, due to GPL freedom in the mask design, various mask can produce the same 3D pattern. The following of this paper is focused on rethinking the mask strategies for an improved exploitation of the photoresist contrast curve in GPL.

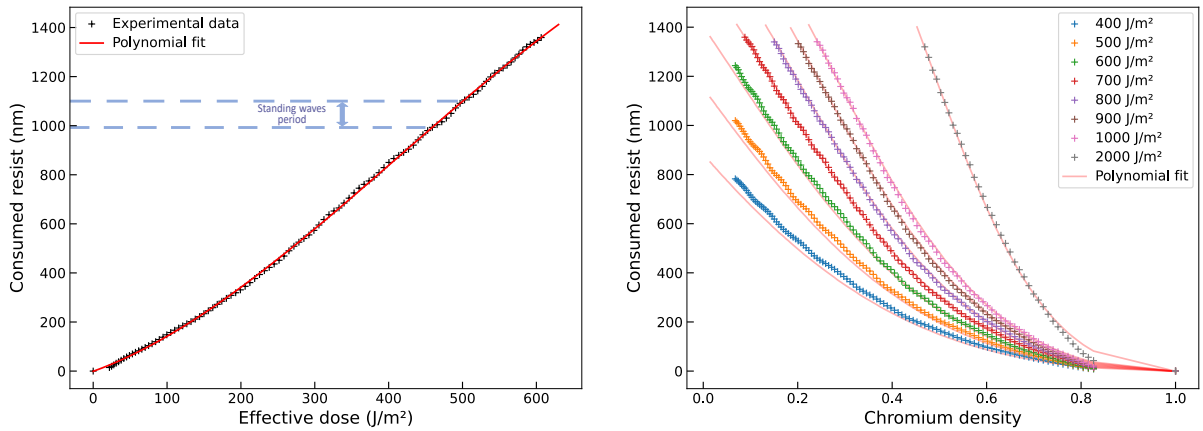

(a) (b)

Figure 6: Contrast curve modelisation and fitting to experimental data (a) for a single dose and (b) extension of the model to other doses conditions

3. VERTICAL RESOLUTION ENHANCEMENT

When it comes to the fabrication of interferential optical filters, one main aspect is the control of the thickness of the used material. For example, in Fabry-Perot cavities, the thickness of the cavity defines the filtered wavelength.

A high claim on the precision of the filtering therefore implies a need for a high resolution process to fabricate the said cavities.

Using GPL and SRF masks, it is possible to ameliorate the vertical resolution by browsing the photoresist contrast curve at the "slowest" possible rate. This can be achieved either by tuning the process itself (stepper dose modulation, development, contrast of the resist), which we will not discuss here, or by considering mask design. The problem becomes as follows, assuming a constant mask writing precision for every patterns : one must find a manufacturable SRF strategy (features shapes, size, arrangement) that allows the smallest possible mask density steps, and therefore the finest possible resist thickness resolution.

One of the main challenge for the mask design is to stay under the resolution limit imposed by Rayleigh's criteria (Eq.6). To do so, the strategy of the repetition of an unitary sub-resolution feature with the pitch itself under the resolution limit comes in handy and is widely found in the literature[6,9–11] (Fig.7).

$$Pitch_{max} = \frac{1}{1+\sigma} * \frac{\lambda}{NA} \tag{6}$$

With $Pitch_{max}$ being the maximum design pitch to stay below the resolution limit, σ the illumination coherence, λ the illumination wavelength and NA its numerical aperture

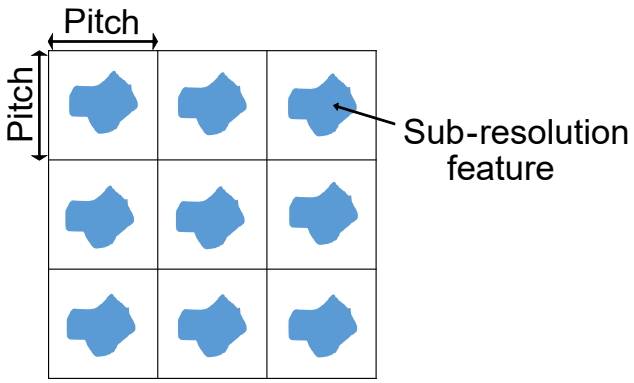

Figure 7: Generic mask design strategy : locking up the chromium features in a grid of pitch value under the resolution limit allows to be compliant with the sub resolution rule

The application of this strategy with chromium "dots" or squares as the sub-resolution feature is the classical scheme. However, we also find the recourse to under-resolved lines[4] and other structures. In fact, one could imagine many mask patterns to fit the specifications. To find the better candidate, we will here consider 6 usecases : dots patterns (positive and negative tone) and lines, each for 2 pitch conditions (200 and 300 nm) (Fig.8). These candidates are chosen for their offer in bigger available density ranges regarding MRC limitations. Indeed, for this study, we consider for the MRC a minimum space of 30 nm and a minimum CD of 40 nm. As an example, to respect such limits at a pitch of 200 nm, the maximum mask chromium density for Fig.8.a is 72.25%, while it would be around 56% if we replace the squares by disks.

For the following part, we make a strong hypothesis on the mask writing precision : for each design the writing precision is equivalent and is of 1 nm per edge. The lithographic process, especially the dose, is also considered constant.

As shown on Fig.9.a, in theory, the contrast curve remains the same for every design strategy. However, the exploited density ranges vary from one design to another due to MRC limitations. These conclusions are also applicable to the modulation of the SRF pitch as experimentally proven on Fig.9.b.

Fig.10 sums up, for each strategy, the available density ranges offered with respect to mask writing rules of minimum feature size of 40 nm, minimum space of 30 nm and a given process, whose dose to clear is here

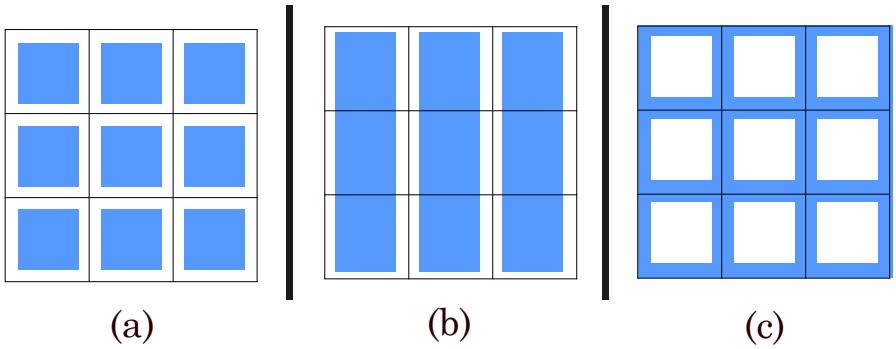

Figure 8: Mask design strategies studycases (a) classical dots strategy, (b) lines strategy, (c) negative tone dots (holes) strategy. Two pitch conditions are investigated for each motif.

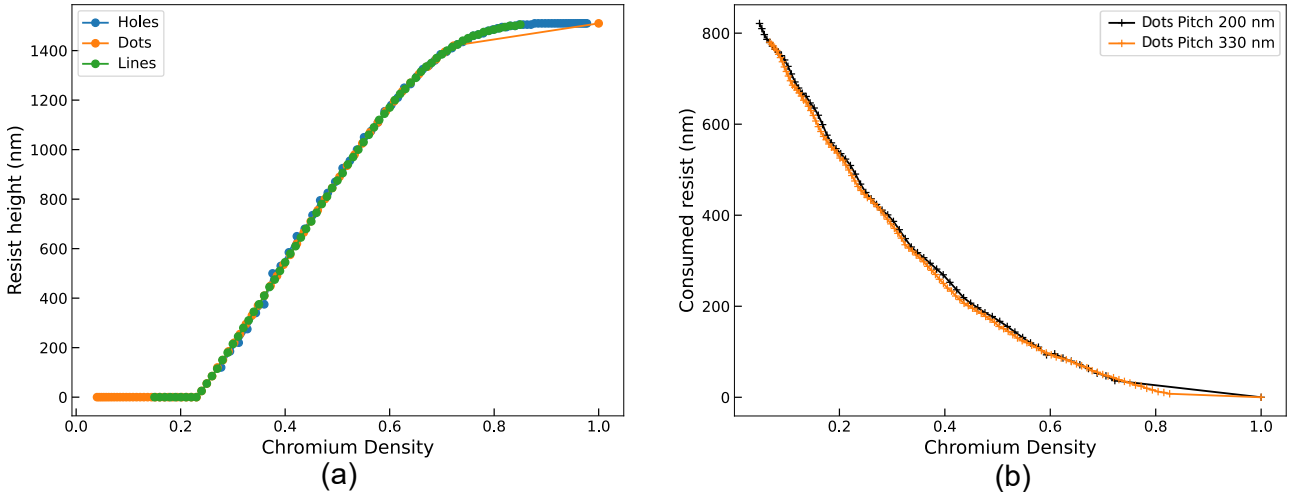

Figure 9: Contrast curves and density ranges permitted by each mask strategies. (a) Shows the theoretical available portion of the photoresist contrast curve for each stategy. (b) Shows the experimental contrast curve for the dots strategy and two different pitch conditions at the dose of 400 J/m^2.

arbitrarily set for a mask chromium density of 0.3. A representative number of accessible densities above the dose-to-clear limit is also indicated with the corresponding mean resolution. The latter represent the available vertical amplitude divided by the number of unique densities : for example, if a strategy allows 10 densities above the dose-to-clear limit and allows the patterning of stairs from 100 to 1000 nm high, the mean resolution would be of 100 nm.

One can easily see the lacks and benefits of each strategy : if the chromium dots strategy is lacking for high densities, the "holes" strategy (negative dots) is suffering for low densities as seen on Fig.10. Lines, however, adopt an average behavior. When it comes to increasing the pitch, this modification has a clear impact of enlarging the density range in both directions for every strategy. Increasing the pitch from 200 nm to 330 nm also allows a neat improvement of the mean resolution as it almost doubles the number of available densities for a unique strategy (112 densities at pitch 200 nm for the lines vs 202 at pitch 300 nm).

These considerations are very straightforward and represent in no way the real limitations regarding the available densities levels or gray levels. Indeed, with a smart design strategy coupling patterns variations (dots, lines, holes) as well as pitch modulations, virtually hundred of thousands of different densities can be obtained. With such freedom on the mask, the limiting aspects regarding the vertical resolution become process related, i.e. the photoresist sensitivity or its inherent rugosity.

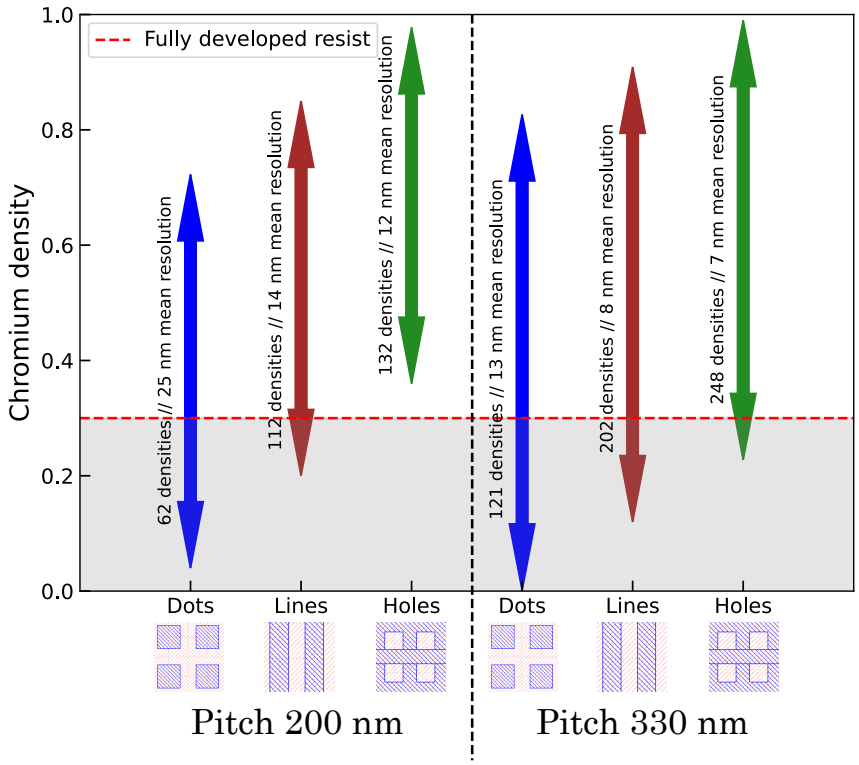

Figure 10: Theoretical density ranges available per mask strategy and indicative mean resolution. Each arrows represent the results for the strategies at a pitch of 200 and 330 nm respectively.

If we demonstrate a high freedom on the mask construction, various considerations can help in choosing the best compromise. Serving this purpose, a status on real maskshop constraints and performances on the writing of every strategy would benefit the study.

Another way of choosing the best strategy, that we will focus on in the next section, is to opt for an improvement of the response to the mask variabilities. In other terms, we are looking for the mask strategy offering the lower MEEF.

4. IMPROVEMENT OF THE RESPONSE TO MASK VARIABILITIES

The degradation of patterned structures due to mask variabilities is a known aspect symbolized by a factor called MEEF (Mask Error Enhancement Factor). Classically, this value indicates the value of an edge placement error (EPE) due to a certain mask writing error. An adapted expression of the MEEF for GPL and its 3D structures has been established in previous studies[8] and illustrates the impact of mask variabilities in different directions :

$$MEEF = \frac{\delta CD_{resist}}{\delta CD_{mask}} = \frac{\delta h_{resist}}{\delta Dens} * \frac{\delta Dens}{\delta CD_{mask}} \tag{7}$$

CD_{resist}, for our case, represents the vertical component and Dens is the mask chromium density. It is then possible to derivate the MEEF from this formula for each of the aforementioned design strategies. Following the same route as previously, we study both the impact of the pitch variation as well as the response of different designs : lines, positive dots and negative dots or holes. Using [7], we can formulate the analytical MEEF for every design strategy.

First, let's take a look at the MEEF response to the pitch variation. We saw previously that increasing the pitch improves vertical resolution, we therefore forecast a similar response for the MEEF. The Fig.11.a depicts the MEEF evolution for the dots design at a constant mask chromium density of 25, 50 and 75 % when varying the pitch. The expected diminution of MEEF with the increment of the pitch is observed and exhibits a non-linear behavior for the dots strategy. This can be explained by the fact that an error on the mask writing at higher pitch would cause a smaller density shift, therefore the MEEF is smaller for higher pitch.

If the pitch increment is an obvious way of diminushing the MEEF, it is less straightforward when it comes to the design variations. It is possible to calculate the analytical MEEF across densities for every strategy using [7]. The Fig.11.b shows the results for each strategies at a pitch of 200 nm; various results are noticeable :

- As shown in previous studies,[8] the MEEF tends to be highly lowered when going for higher densities
- Each strategy has a different behavior and extremum. Depending on the aimed density, one strategy may be preferred to another. However, the lines strategy tends to produce better MEEF overall.

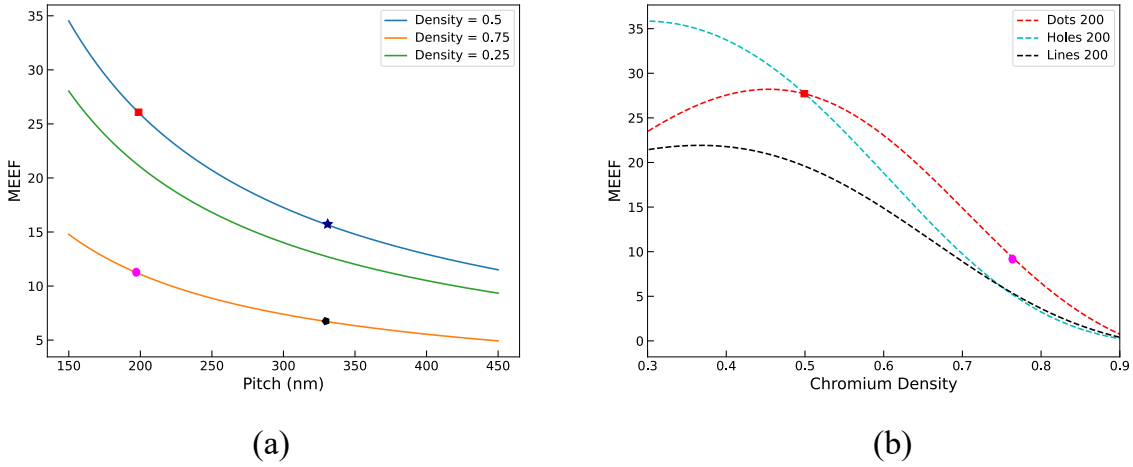

Figure 11: MEEF evolution for different design considerations. Each small pattern corresponds to a single design configuration in (a), (b) and Fig.12. As an exemple, the blue star corresponds to the dots strategy at a pitch = 330 nm and a chromium density of 0.5 (a) Exhibits the diminution of MEEF for the dots design strategy when increasing the pitch and keeping a constant chromium density. (b) depicts the MEEF against density for the three design patterns strategies.

Fig.12 present the MEEF variation against density when considering both of the previous studies : design modulations and pitch variations.

We can see that almost every strategy at pitch = 330 nm exhibits even or lower MEEF than the lines at a pitch = 200 nm for the considered density range. This shows how the pitch plays a huge role in lowering the MEEF by almost halving its values for this case. With these results, we show that we are able to noticeably reduce MEEF with an appropriate and smart design strategy, i.e. in our example by the recourse to higher pitch and lines design strategy. However, one should be careful with these methods, in particular regarding the pitch increase. Indeed, we know that the pitch must be chosen to stay in a non-resolved system. Moreover, this restriction is even stricter for the lines strategy : in theory, every SRF strategy exhibit the same maximum pitch limit according to [6] to stay non-resolved. When flirting with this limit however, the contrast of the transition from non-resolved to resolved is way bigger for the lines strategy than for the dots strategy as shown on Fig.13. This figure represent the variation in intensity of the aerial image for a constant mask chromium

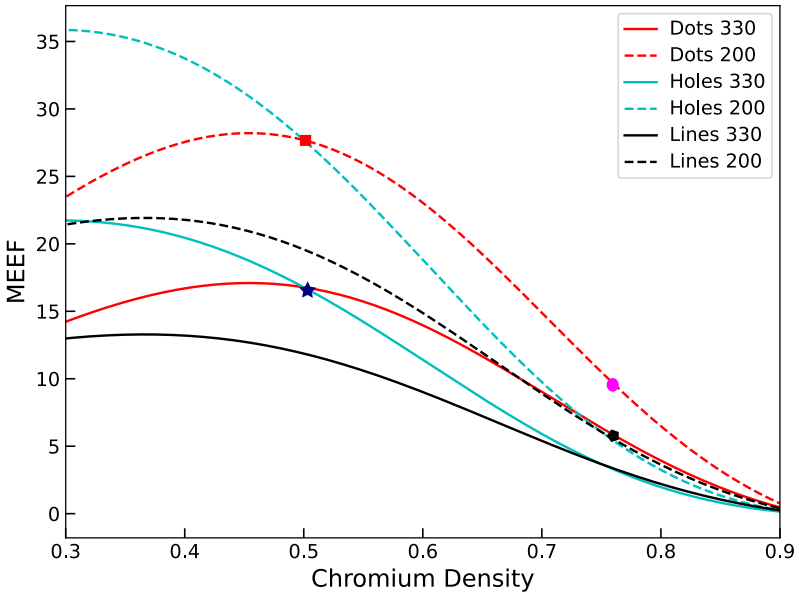

Figure 12: MEEF response to mask features shapes variations and pitch modulation.

density at different pitch conditions. As the chromium density is constant, the aerial image should be flat for a non-resolved mask and exhibit no variations. When increasing the pitch, whenever variations appear in the aerial image intensity the chromium patterns are beginning to print. We can see by simulation that for both the dots and lines strategies the printing is starting at a pitch of around 380 nm for our configuration. However, the amplitude of this phenomenon is larger for the lines than for the dots. This means that in practice, for a unique pitch condition around the resolution limit, the partial resolution of the lines design would be more noticeable than the dots design.

Another aspect that shouldn't be ignored is the maskshop capability, as some designs might offer an inherent lower writing variability and therefore a naturally lower MEEF impact.

5. CONCLUSIONS AND PERSPECTIVES

In the world of 3D micro-fabrication, grayscale photolithography is one of the leading patterning method at the industrial scale. The method relies on a low contrast photoresist and non-resolved binary mask to perform the fabrication of the 3D components. In this study, we have shown that plural mask dataprep strategies are available, each one exhibiting different performances depending on the aimed application.

The study vehicle is a straircase like structure composed of Fabry-Perot cavities of varying height. Such an application requires a high resolution and control over the vertical component. To answer these specifications, we firstly produced a contrast curve modelisation of the low contrast photoresist. Then, we investigated various mask design strategies. Both the choice of the mask sub-resolution features (dots, lines, holes) and their arrangement (pitch) are shown to impact the mask performances. Within the litterature, the dots structure is widely found for grayscale patterning. However, we demonstrated here that for our application, the recourse to non-resolved lines at a high pitch offers a better vertical resolution and sturdiness regarding the MEEF. Nevertheless, a special attention should be allowed to staying in a non-resolved grayscale regime.

For other applications, different strategies might be preferable. As an example, for the fabrication of microlenses, a mask composed of concentric rings may be a best choice. In conclusion, when patterning 3D structures using GPL, one should question the mask strategy to benefit in performance from the freedom allowed on the mask design. This demonstrated freedom on the mask design also indicates that the actual limitations for GPL

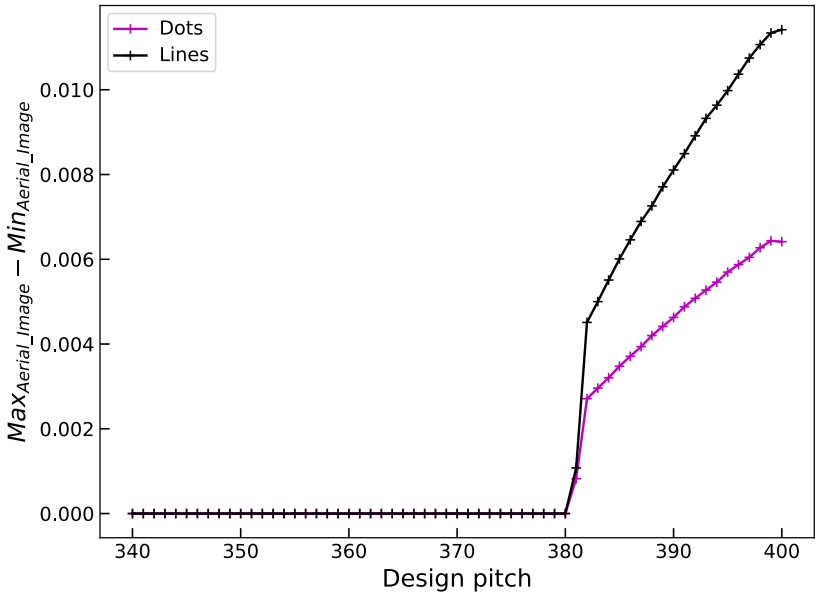

Figure 13: Aerial image intensity variation against pitch for a constant chromium density unitary design : variation in the aerial image indicates the beginning of the resolution of the mask patterns.

regarding the vertical resolution do not come from the mask itself. Indeed, the process itself become the limiting aspect due to its variability or its inherent rugosity. Accordingly, efforts regarding the lithographic process are the main remaining improvable area.

Moreover, during this work, we omitted several aspects that could be studied to go further. First, we worked with a fixed mask writing precision, equivalent for every strategy. A status on strategy-wise maskshop writing performances and higher mask grades would be relevant.

Then, we considered large stairs and therefore ignored the transition bewteen two of them. The impact of this transition on the final product performance would be of interest. In the same field, considering the recourse of 248 nm lithography tools to optimize the lateral resolution of GPL could also benefit further studies. However, the counterpart of going for shorther wavelength would be a lowered pitch to stay under the resolution limit.

REFERENCES

[1] Kirchner, R. and Schift, H., "The ascent of high resolution and high volume 3d replication," *Microelectronic Engineering* **141**, 243–244 (jun 2015).

[2] Li, X., Yu, S., Gui, C., and Sun, C., "Novel three-dimensional 90° bend waveguides with high optical transmission efficiency based on silicon-on-insulator," *Photonics and Nanostructures - Fundamentals and Applications* , 101181 (2023).

[3] Microlight3D, "Two-photon polymerization technology," *Online archive* (Consulted 28/11/2023).

[4] Schneider, J., Kaiser, D., Morgana, N., Heller, M., and Feick, H., "Revival of grayscale technique in power semiconductor processing under low-cost manufacturing constraints," in [*34th European Mask and Lithography Conference*], Behringer, U. F. and Finders, J., eds., **10775**, 107750W, International Society for Optics and Photonics, SPIE (2018).

[5] Williams, C., Gordon, G. S. D., Wilkinson, T. D., and Bohndiek, S. E., "Grayscale-to-color: Scalable fabrication of custom multispectral filter arrays," *ACS Photonics* **6**, 3132–3141 (oct 2019).

[6] Chevalier, P., Quemere, P., Berard-Bergery, S., Henry, J.-B., Beylier, C., and Vaillant, J., "Rigorous model-based mask data preparation algorithm applied to grayscale lithography for the patterning at the micrometer scale," *Journal of Microelectromechanical Systems* **30**, 442–455 (jun 2021).

[7] Pierre, C., Quéméré, P., Beylier, C., Berard-Bergery, S., Allouti, N., Paris, M., Farys, V., and Vaillant, J., "Beyond contrast curve approach: a grayscale model applied to sub-5µm patterns," 49 (03 2019).

[8] Palanchoke, U., Bélot, G., Bérard-Bergery, S., Saugnier, J., Sungauer, E., Beylier, C., Tomaso, F., Pourteau, M.-L., Mendes, I., Coquand, R., and Bernadac, A., "Mask errors impact on grayscale lithography patterning," in [*Novel Patterning Technologies 2023*], Liddle, J. A. and Ruiz, R., eds., **12497**, 124970N, International Society for Optics and Photonics, SPIE (2023).

[9] Oppliger, Y., Sixt, P., Stauffer, J., Mayor, J., Regnault, P., and Voirin, G., "One-step 3d shaping using a gray-tone mask for optical and microelectronic applications," *Microelectronic Engineering* **23**, 449–454 (jan 1994).

[10] Yao, J., Su, J., Du, J., Zhang, Y., Gao, F., Gao, F., Guo, Y., and Cui, Z., "Coding gray-tone mask for refractive microlens fabrication," *Microelectronic Engineering* **53**, 531–534 (jun 2000).

[11] Kusar, P., Jessenig, S., and Eilmsteiner, G., "Single mask step etching of fabry–pérot etalons for spectrally resolved imagers," *Journal of Micromechanics and Microengineering* **30**, 085004 (jun 2020).